First-order liquid crystal orientation transition on inhomogeneous substrates

Ophelia K. C. Tsui,* Fuk Kay Lee, Baoshe Zhang, and Ping Sheng
Department of Physics and Institute of Nano Science and Technology, Hong Kong University of Science and Technology, Clear Water Bay, Kowloon, Hong Kong

(Received 28 October 2003; published 24 February 2004)

In a recent experiment, we uncovered an unconventional liquid crystal (LC) orientation transition on microtextured substrates consisting of alternating horizontal and vertical corrugations. When the period of alternation was decreased toward ~ 1 μm, the LC alignment underwent an abrupt transition from inhomogeneous planar to a more uniform configuration with a large pretilt angle ($\sim 40°$). With the aid of a model based on the competition between the Frank-Oseen elastic energy and a phenomenological surface potential of the form $W(\theta,\phi)=(1/2)W_\theta^{(2)}\sin^2\theta+(1/4)W_\theta^{(4)}\sin^4\theta+(1/2)W_\phi\cos^2\theta\sin^2\phi(x,y)$ (where θ and ϕ are, respectively, the pretilt and azimuthal angles of the LC director and $W_\theta^{(2)}$, $W_\theta^{(4)}$, and W_ϕ are constants) that demonstrated good agreement with experiment, we investigated the microscopic origin of the observed transition. It was found that this transition comprises two steps. First, the LC director homogenizes toward the $\phi=45°$ azimuthal direction in the plane to relax the elastic energy. The resulting rise in azimuthal anchoring energy subsequently drives the LC to adopt a finite pretilt. The values of the W's deduced from the model reveal that the polar anchoring energy is about $\sim 1/10$ of the typical values, with the $\sin^4\theta$ term dominating the $\sin^2\theta$ term. We present a possible explanation for this unexpected finding.

DOI: 10.1103/PhysRevE.69.021704 PACS number(s): 61.30.Hn, 61.30.Eb, 61.30.Dk

I. INTRODUCTION

Conventional techniques for uniform liquid crystal (LC) alignment such as rubbing, oblique evaporation of silicon oxide, and surfactant treatment produce alignment effects that are uniform on the substrate surface. Recently, increasing effort has been spent on the use of patterned substrate surfaces with spatially varying easy alignment directions to achieve uniform LC alignment [1–7], since it has been demonstrated that the resulting LC alignment is applicable to bistable displays [5,6], and that the patterned surfaces may allow for complete control of LC orientation direction [7]. In the initial proposal by Ong *et al.* [1], the inhomogeneous substrate pattern induces a spatially varying LC director field for the molecular layer of LC immediately next to the substrate surface, which, however, decays exponentially to uniform alignment with a decay length $\cong\lambda/2\pi$ where λ is the periodicity of the substrate pattern. Operationally, the inhomogeneous substrate together with the boundary layer of LC (within a few decay lengths from the substrate) can be viewed as providing uniform anchoring for the *bulk* LC with an effective homogeneous surface potential that in turn depends on the local anchoring energies of the patterned surface and the LC elastic constants [1]. By using the Frank-Oseen form for the LC elastic energy [8], Barbero *et al.* [9] obtained analytical expressions for the effective bulk LC direction and effective surface potential for surfaces patterned with stripes of alternating easy directions and anchoring energies. In a more recent study, Qian and Sheng [2,10] examined the problem within the Landau–de Gennes framework and found that the LC underwent a first-order orientational transition from an inhomogeneous state to a uniform alignment configuration as the pattern periodicity was decreased below the LC elastic correlation length inherent to the Landau–de Gennes formalism. In all these prior theoretical investigations [2,9,10], only substrate patterns consisting of parallel stripes of varying preferred polar orientations θ_0 were considered. But the majority of recent experiments [4–7] have studied checkerboard patterns with varying preferred azimuthal alignment ϕ_0, with the preferred polar orientation fixed at 0°. In particular, a recent experiment by us [7] showed that a LC orientation transition can occur as the periodicity of such checkerboard pattern is decreased, in which the inhomogeneous state changes to a uniform alignment state possessing a large pretilt angle.

In this paper, we present a detailed theoretical investigation of the equilibrium LC alignment states associated with this experiment. Our study is based on the Frank-Oseen framework on checkerboard substrate patterns of varying periodicities with alternating 0° and 90° preferred azimuthal alignment. For such patterned substrates, we assume the potential to have the commonly adopted form [1,4,11,12]

$$W(\theta,\phi)=\frac{1}{2}W_\theta^{(2)}\sin^2\theta+\frac{1}{4}W_\theta^{(4)}\sin^4\theta+\frac{1}{2}W_\phi\cos^2\theta\sin^2[\phi-\phi_0(x,y)], \quad (1)$$

where $W_\theta^{(2)}$ and $W_\theta^{(4)}$ account for the polar anchoring strength [1,11] and W_ϕ the azimuthal anchoring strength [4,12] of the substrate on the LC. Excellent agreement was found between the results of this model and experimental observations of different groups [4,7].

The organization of this paper is as follows. In Sec. II, we summarize our findings about the equilibrium LC states from this theoretical modeling. In Sec. III, we describe the model in detail, followed by presentations of the simulation results and discussion in Sec. IV. We conclude with a few observations in Sec. V.

*Author to whom correspondence should be addressed.

II. SUMMARY OF FINDINGS

Our model calculations were found to reproduce and allow for reconciliation between the experimental findings of different groups [4,7]. When W_ϕ is large so that all the pattern periodicities examined are greater than $\sim k_{11}/W_\phi$ (where k_{11} is the LC splay elastic constant), an inhomogeneous alignment state with the effective easy direction along $(\theta,\phi)=(0°,45°)$ persists. This prediction is consistent with the result of Kim *et al.* on inhomogeneous checkerboard patterns produced by nanorubbing [4], in which no LC orientation transition was observed. But if W_ϕ is such that some patterns have periodicity comparable to k_{11}/W_ϕ, an unexpected LC orientation transition may occur. In this case, the azimuthal anchoring strength of an individual domain is not strong enough to overcome the rigidity of the LC director against bending and splay deformations. Hence, substantial relaxation of the director toward the $\phi=45°$ symmetry direction can take place. If in addition $W_\phi > \sim 2W_\theta^{(2)}$, the increase in azimuthal surface energy due to this relaxation can be large enough to trigger a first-order orientation transition to a (more) uniform state with a finite pretilt. This prediction was realized in a recent experiment [7] on microtextured substrates with topographic features produced by atomic force microscopic (AFM) local oxidation [14]. The magnitude of W_ϕ obtained by fitting to experiment agrees with estimates from prevalent theory [12]. However, $W_\theta^{(2)}$ is at least an order of magnitude smaller than typical values. We further deduced that $W_\theta^{(4)}$ is greater than $W_\theta^{(2)}$, which deviates from the Rapini-Papoular potential [13]. This unconventional finding for the polar anchoring potential is attributed to the unique setting of a checkerboard surface pattern on which the LC director undertakes significant relaxations toward the $\phi=45°$ direction. The resulting polar anchoring energy is thus measured from the $\phi=45°$ direction, far removed from the $\phi=0°$ direction as in conventional circumstances. Simple reasoning shows that this can lead to a reduction in $W_\theta^{(2)}$ and to the need for a higher-order term in the polar anchoring energy.

III. THE MODEL

The substrate patterns considered in this study are shown in Fig. 1, which were the same ones used in the experiment of Ref. [7]. As seen, the patterns are composed of alternating x and y corrugations 85 nm (wide)×30 nm (height) with variable periodicity λ. We consider a semi-infinite space filled with nematic LC above a surface at $z=0$ as shown in Fig. 1. The inhomogeneous anchoring property of the surface is simulated by the potential given by Eq. (1), with the local easy azimuthal direction $\phi_0(x,y)$ varying according to

$$\phi_0(x,y)=\begin{cases} 0° & \text{if } 0\leqslant x\leqslant m+\dfrac{\lambda}{2} \text{ and } 0\leqslant y\leqslant m+\dfrac{\lambda}{2} \text{ or} \\ & m+\dfrac{\lambda}{2}\leqslant x\leqslant (m+1)\lambda \text{ and } m+\dfrac{\lambda}{2}\leqslant y\leqslant (m+1)\lambda \\ & \text{where } m=0,1,2,\ldots, \\ 90° & \text{otherwise.} \end{cases}$$

The LC elastic energy $U_{\rm el}$ in the Frank-Oseen form [8] is

$$U_{\rm el}=\int d^3r\frac{1}{2}\{k_{11}(\boldsymbol{\nabla}\cdot\boldsymbol{n})^2+k_{22}(\boldsymbol{n}\cdot\boldsymbol{\nabla}\times\boldsymbol{n})^2 + k_{33}(\boldsymbol{n}\times\boldsymbol{\nabla}\times\boldsymbol{n})^2\}, \quad (2)$$

where **n** is the LC director, and k_{11}, k_{22}, and k_{33} are the splay, twist, and bend elastic constants, respectively. We assume the parameters to take the values relevant to the nematic LC 4′-*n*-pentyl-4-cyanobiphenyl (5CB), i.e., $k_{11}=7\times10^{-12}$ N, $k_{22}=3.5\times10^{-12}$ N, $k_{33}=1\times10^{-11}$ N [15]. The total energy of the system, $U_{\rm tot}$, is given by

$$U_{\rm tot}=U_{\rm el}+U_{\rm S}, \quad (3)$$

where

$$U_{\rm S}=\int d^3r\,W(\theta,\phi)\,\delta(z) \quad (4)$$

is the surface energy. In Eq. (4), $\delta(z)$ is the one-dimensional delta function and $W(\theta,\phi)$ is given by Eqs. (1) and (2). The equilibrium LC state is determined by the director configuration $\boldsymbol{n}(\boldsymbol{r})=(\theta(\boldsymbol{r}),\phi(\boldsymbol{r}))$ that minimizes $U_{\rm tot}$. The minimization was performed for unit cells of thickness λ/2 and 0.2 μm≤λ≤80 μm. The integration volume was discretized into 14×14 points in the x-y plane (so the discretization step =λ/14) and 30 points in the z direction (corresponding discretization step=λ/60). Doubling either of the two numbers of discretization points or the integration cell thickness produced less than 1% variation in the calculated energy. The LC director's polar and azimuthal angles [respectively, $\theta(\boldsymbol{r}_i)$ and $\phi(\boldsymbol{r}_i)$] at all discretization points $\boldsymbol{r}_i$ ($i=1,2,\ldots,5880$) were treated as independent variables with respect to which $U_{\rm tot}$ was minimized by the conjugate gradient method as in Ref. [2]. To ensure that the energy of the state obtained was the global minimum, several random starting configurations were used at the smallest (or largest) λ considered. Then the resultant optimal configurations were used as the starting

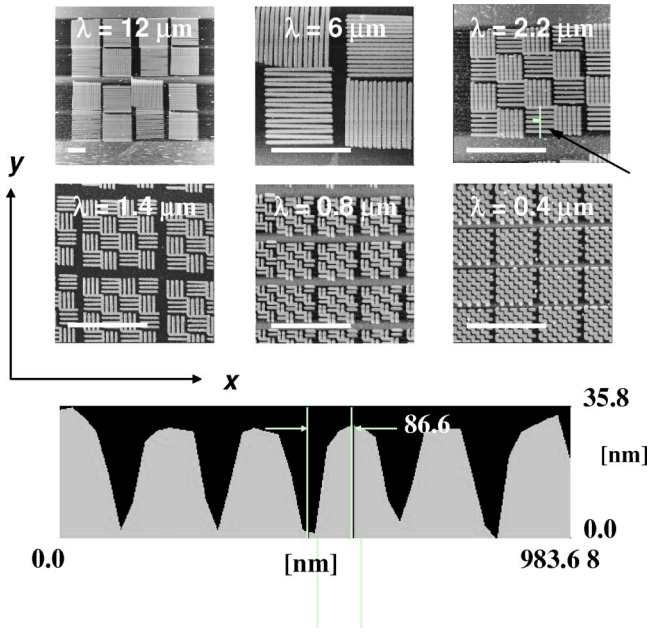

FIG. 1. AFM topographical images of microtextured substrates used in the experimental study of Ref. [7]. These substrates were fabricated by AFM local oxidation [14]. The scale bars are 3 μm. The arrow in the $\lambda=2.2$ μm sample indicates from where the cross-sectional profile in the lower panel was drawn.

configurations for the next higher (or smaller) λ considered. This continuation method may thus generate several curves of local minimum $U_{\rm tot}$ as a function of λ. We found that except near the orientation transition, if any, the curves were independent of whether we performed the calculation in an increasing or decreasing order of λ. Furthermore, the curves obtained from different starting configurations give rise to at most two branches — one with $\langle\theta\rangle=0°$ and the other with $\langle\theta\rangle=40°$, with the branching occurring also only near the orientation transition.

IV. RESULTS AND DISCUSSIONS

We consider a surface potential $W(\theta,\phi)$ that gives rise to a LC alignment transition like that observed in Ref. [7], i.e.,

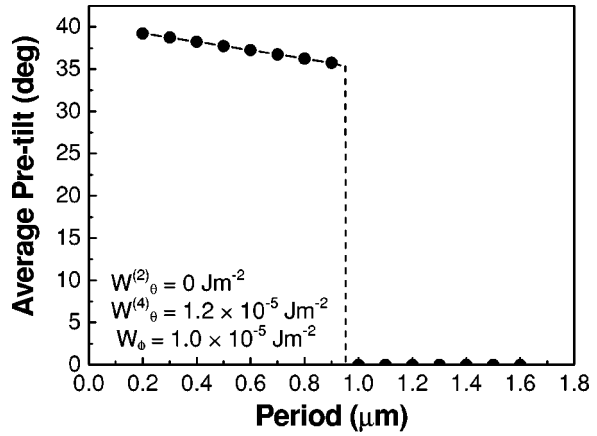

FIG. 2. Average LC pretilt as a function of pattern periodicity obtained by using parameters for the surface potential [Eq. (1)] as indicated.

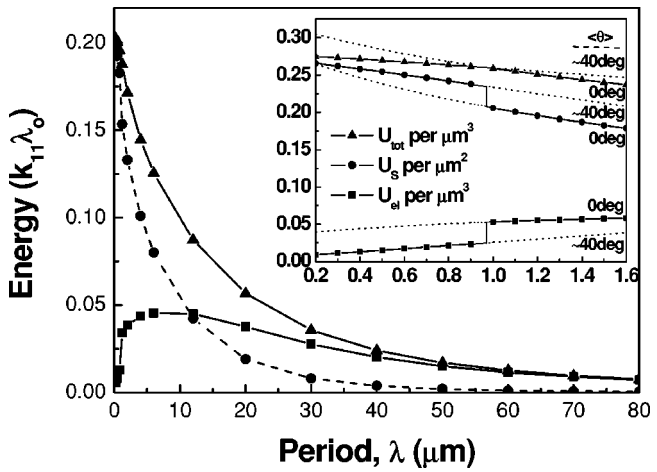

FIG. 3. (Main panel) Variations of the calculated $U_{\rm tot}$, $U_{\rm el}$, and $U_{\rm S}$ versus pattern periodicity. Here, $\lambda_0\equiv 1$ μm. (Inset) The same plot as in the main panel except that it is focused on the region of λ near the orientational transition. The dotted lines depict the energies of the metastable states. The calculation assumed the same surface potential used to generate the data of Fig. 2.

θ demonstrated an abrupt jump from 0° to 40° when λ was decreased toward ~1 μm. It has been noted [7] that the transition can be reproduced with the present model if the surface potential parameters satisfy the following criteria:

$$W_\phi=\gamma W_\theta^{(4)}/2$$

and

$$W_\theta^{(2)}=(0.5-0.8435/\gamma)W_\phi(\gamma\geqslant 1.687). \tag{5}$$

The origin of these criteria will become apparent after we show how the elastic energy, surface energy, and director field of the LC vary across the orientation transition. We use a particular choice of the surface potential to exemplify variations of these specific properties. Figure 2 shows a plot of average pretilt angle versus pattern periodicity obtained for the choice with $W_\theta^{(2)}=0$, $W_\theta^{(4)}=1.2\times10^{-5}$ J m^{-2}, and $W_\phi=1.0\times10^{-5}$ J m^{-2} [7]. As seen, there is an orientation transition displaying a 40° jump in θ at $\lambda\approx1$ μm. We then examine variations of the calculated $U_{\rm tot}$, $U_{\rm el}$, and $U_{\rm S}$ as a function of λ over 0.2 μm$\leqslant\lambda\leqslant$80 μm. From Fig. 3, one can see that, on decreasing λ from 80 μm, $U_{\rm el}$ shows a slow rise initially, but starts to decrease rapidly with decreasing λ near $\lambda=5$ μm. The latter behavior is contrary to the simplistic expectation with the form of $U_{\rm el}$ shown in Eq. (2). On the other hand, $U_{\rm S}$ demonstrates a much more rapid and monotonic rise with decreasing λ, and begins to match $U_{\rm tot}$ closely below $\lambda=5$ μm (where $U_{\rm el}$ shows the onset of a fall). In the vicinity of the orientation transition (inset of Fig. 3), however, variations in the three energies, i.e., $U_{\rm tot}$, $U_{\rm el}$, and $U_{\rm S}$, are much more gentle except at $\lambda=1.05$ μm, where $U_{\rm el}$ and $U_{\rm S}$ show a jump and $U_{\rm tot}$ shows a discontinuous change in slope, exemplifying a first-order phase transition.

We first try to understand the onset of the decrease in $U_{\rm el}$ around $\lambda=5$ μm. In regions on the $z=0$ plane between domains containing the x corrugations and the y corrugations,

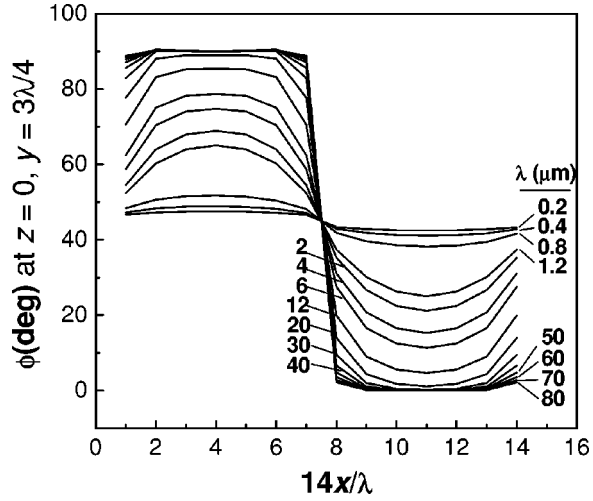

FIG. 4. Profiles of $\phi(x)$ at $z=0$ and $y=3\lambda/4$ for different values of λ between 0.2 and 80 μm.

we expect the azimuthal alignment of the LC to undergo a gradual transition from the $\phi=0°$ orientation to the $\phi=90°$ orientation (domain wall). If λ is not much larger than the extrapolation length [16], the azimuthal alignment can deviate significantly from the local easy direction in the domain, causing considerable relaxation of the director field in the plane. The extrapolation length is a weighted sum of k_{11}/W_ϕ ($=0.64$ μm) and k_{33}/W_ϕ ($=0.91$ μm) [16]. Therefore, azimuthal relaxation of the LC director can very well commence at the noted value of λ (≈ 5 μm) where $U_{\rm el}$ starts to decline with decreasing λ, which is a few times the extrapolation length. Figure 4 displays the profiles of $\phi(x)$ along the line $y=3\lambda/4$ at $z=0$ for various values of λ up to 80 μm. Consistent with the onset of the fall in $U_{\rm el}$, the deviation of ϕ from ϕ_0 at the domain center also becomes significant ($>10°$) near $\lambda=6$ μm, although the deviation actually begins as soon as $\lambda\leqslant 30$ μm. The latter is in keeping with the onset of a rise in $U_{\rm S}$ around $\lambda=30$ μm in the main panel of Fig. 3. For still larger values of λ (>30 μm), the slow increase in $U_{\rm S}$ with decreasing λ may arise from the misalignment of the LC director from ϕ_0 in the domain wall region between the two types of domains. Another interesting feature to note from Fig. 4 is the abrupt flattening of $\phi(x)$ between $\lambda=0.8$ μm and 1.2 μm, which coincides with the location of the orientational transition revealed by Fig. 2 and the inset of Fig. 3. Flattening of $\phi(x)$ signifies a qualitative improvement in the uniformity of the LC configuration in the plane. To better see this change of the LC alignment, we display the two-dimensional projection of the LC director in the x-y plane at $z=0$ for $\lambda=1.1$ μm (above the transition) and $\lambda=0.2$ μm (below the transition) in Figs. 5(a) and 5(b), respectively. For the LC configuration with $\lambda=1.1$ μm, the deviation of the director azimuth from the preferred azimuth (i.e., $\sqrt{\langle(\phi-\phi_0)^2\rangle}$, where ϕ_0 is the angle with the lowest azimuthal surface potential) is 33°, and the corresponding spread in the distribution of ϕ (i.e., $\sqrt{\langle(\phi-\langle\phi\rangle)^2\rangle}$ is 16°. But for the configuration with $\lambda=0.2$ μm, the values of the two corresponding parameters are 44° and 1°, respectively. The finding that the state for $\lambda=0.2$ μm is more uniform

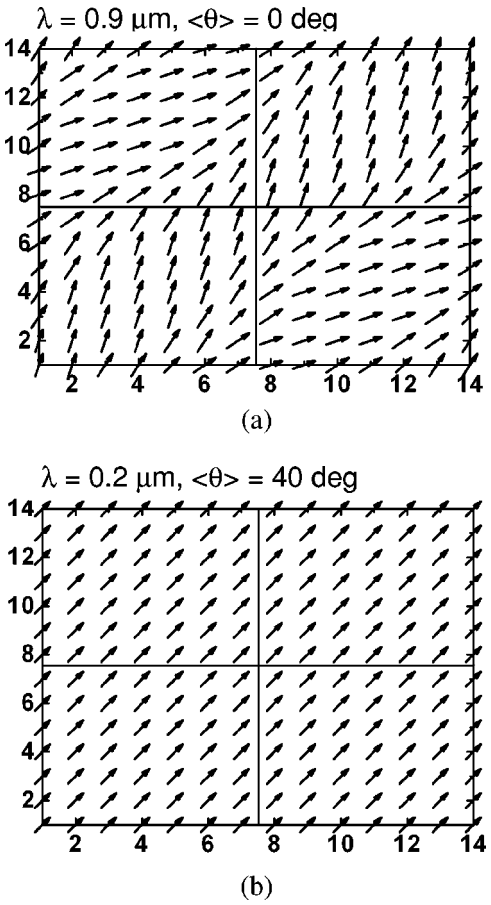

FIG. 5. Projections of the LC director in the x-y plane at $z=0$ for λ equals (a) 1.1 μm and (b) 0.2 μm. Data are presented for one unit cell. The x and y scales are in units of discretization steps.

than its counterpart for $\lambda=1.1$ μm corresponds well with its lower elastic energy as illustrated by the inset to Fig. 3. The higher surface energy of the $\lambda=0.2$ μm state comes from its larger value of $\langle\theta\rangle$, plus the larger rms deviation of ϕ from ϕ_0. We now examine the factor(s) that determine the pretilt orientation of the LC director. Some insights may be gained by examining plots of the surface potential $W(\theta,\phi)$ as a function of θ for various fixed values of $|\phi-\phi_0|$. As seen from Fig. 6, when $|\phi-\phi_0|$ is increased, the position of the $W(\theta,\phi)$ minimum, $\theta_{\rm min}$, gradually shifts from 0° to larger values and eventually reaches 40° when $|\phi-\phi_0|$ is equal to 45°. In the meantime, the depth of the minimum increases and so does the value of $W(0°,\phi)$. With these noted variations in the surface potential with increasing $|\phi-\phi_0|$, we can envision a picture for the occurrence of the LC orientation transition. When the pattern periodicity is decreased, $\langle|\phi-\phi_0|\rangle$ increases while the spread of $\phi(\boldsymbol{r})[=\sqrt{\langle(\phi-\langle\phi\rangle)^2\rangle}]$ decreases. At some point, the surface energy of the inhomogeneous state $[=\langle W(0°,|\phi-\phi_0|)\rangle]$ becomes $\approx W(0°,\langle|\phi-\phi_0|\rangle)$. When compared with the surface energy of the uniform state represented by $\theta=\theta_{\rm min}$ and $\langle\phi\rangle\cong\phi_0\pm 40°$ $[\approx W(\theta_{\rm min},|\langle\phi\rangle-\phi_0|\cong 40°)]$ [7], the difference might become smaller than their corresponding elastic energy difference $\Delta U_{\rm el}$, thereby making the orientation transition energetically feasible. Fig-

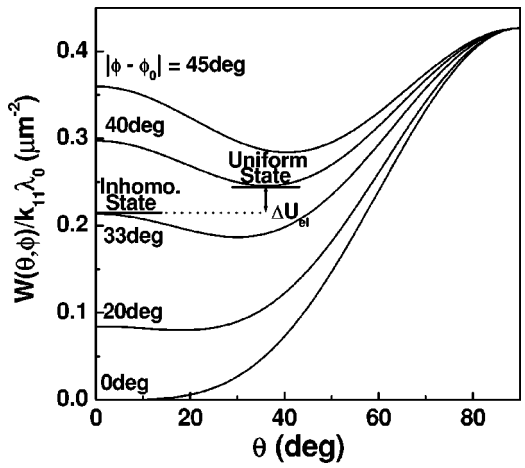

FIG. 6. $W(\theta,\phi)$ vs θ for various fixed values of $|\phi-\phi_0|$ as indicated. Here, $\Delta U_{\rm el}$ denotes the difference in elastic energy between the inhomogeneous and uniform state. It is put here to demonstrate the balance of energy for the orientation transition.

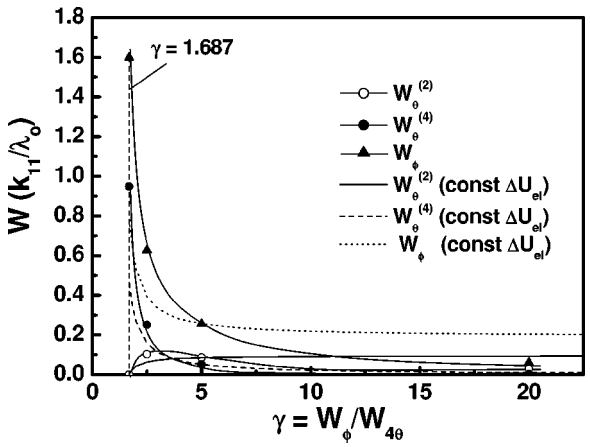

FIG. 7. Various surface energy parameters that were found to reproduce the LC orientation transition observed in Ref. [7] when applied to the model calculations. Those parameters labeled by "(const $\Delta U_{\rm el}$)" are calculated by using Eq. (5) and assuming the change in elastic energy at the transition to be constant, fixed to that found for $\gamma=5$.

ure 6 illustrates this point. It is interesting to note that the sizes of the surface energies of the two states and of $\Delta U_{\rm el}$ deduced by this simple-minded consideration agree quite well with the corresponding quantities found by numerical simulations (inset of Fig. 3). It should, however, be remarked that this way of deducing the balance of energy is expected to fail should the spread in ϕ too large, so that the surface energy of the single director state $=W(0°,\langle|\phi-\phi_0|\rangle)$ can no longer provide a good approximation for the actual surface energy of the inhomogeneous state. The present finding suggests a simple way of setting the criterion for $W(\theta,\phi)$ that may give rise to a LC orientation transition from a planar inhomogeneous alignment state to a more uniform alignment state with a given pretilt. According to Fig. 6, $W(\theta,\phi)$ should possess a minimum at the desired pretilt angle of the uniform state when $|\phi-\phi_0|=45°$. In fact, it was by application of this requirement to Eq. (1) that we derived the two criteria given by Eq. (5). Nonetheless, these two criteria alone are not sufficient to determine all three parameters $W_\theta^{(2)}$, $W_\theta^{(4)}$, and W_ϕ. One more criterion is required, namely, the orientation transition should occur at the desired value of λ. For this study, the desired value is ~ 1.1 μm to match the result of Ref. [7]. Figure 7 shows the surface energy parameters that have been found to reproduce the observed transition [7]. In the same graph are displayed the corresponding parameters (represented by line curves) estimated by using Eq. (5) and assuming $\Delta U_{\rm el}$ to be a constant equal to that found for $\gamma=5$. As seen, while the surface energy parameters thus obtained demonstrate qualitatively similar dependencies on γ as those actually found, there are systematic deviations suggesting that $\Delta U_{\rm el}$ decreases with increasing γ. Since γ is the ratio of W_ϕ to $W_\theta^{(4)}/2$, this observation suggests that the surface energy difference at the transition decreases with increasing $W_\phi/W_\theta^{(4)}$.

From Fig. 7, it is seen that W_ϕ is always larger than both $W_\theta^{(2)}$ and $W_\theta^{(4)}$, which is contradictory to what was typically found. Another unusual observation is that $W_\theta^{(4)}$ either dominates (for $\gamma<3$) or else is comparable to $W_\theta^{(2)}$, violating the commonly obtained Rapini-Papoular (RP) potential $W_{\rm RP}\sim(\boldsymbol{n}\times\boldsymbol{n}_0)^2$ [13], where $\boldsymbol{n}=(\theta,\phi)$, and $\boldsymbol{n}_0=(\theta_0,\phi_0)$ is the easy direction. Since $k_{11}/\lambda_0=0.7\times10^{-6}$ J/m^{-2}, the range of W_ϕ found (i.e., $\leqslant 1.1\times10^{-5}$ J/m^{-2} according to Fig. 7) encompasses the prediction from Berreman's model (which is $W_\phi\cong 1\times10^{-5}$ J/m^{-2}) [12]. If we let $W_\phi=1.1\times10^{-5}$ J/m^{-2}, we face the anomaly that $W_\theta^{(4)}$ is about ten times smaller than reported values [11] However, it is noteworthy that in typical surface anchoring energy measurements one either keeps $\theta=\theta_0$ and measures the variations in surface energy as a function of $(\phi-\phi_0)$, or maintains $\phi=\phi_0$ and measures the surface energy as a function of $(\theta-\theta_0)$. With these measurement schemes, one obtains W_ϕ and $W_\theta^{(2)}$, respectively. In the LC orientation transition presently considered, an unusual circumstance is encountered, i.e., one is considering the polar anchoring energy for the case in which the LC director deviates from the usual $\phi=\phi_0$ direction. To see how this different setting may affect the measured polar anchoring energy, we rewrite the general form of $W_{\rm RP}$ as

$$W_{\rm RP}\sim\sin^2(\phi-\phi_0)+\cos^2(\phi-\phi_0)\sin^2(\theta-\theta_0). \qquad (6)$$

From Eq. (6), the coefficient of $\sin^2(\theta-\theta_0)$ diminishes as $|\phi-\phi_0|$ increases, reaching 0 when $|\phi-\phi_0|=90°$. But this limit of the polar energy is unphysical since it predicts that the polar anchoring energy should become independent of θ. It shows that the RP potential needs to be adjusted when $|\phi-\phi_0|$ is large. From the above discussion, we expect $W_\theta^{(2)}$ to be diminished and a nontrivial higher-order term such as $\sin^4(\theta-\theta_0)$ to emerge. Both have been found in this case.

We also examine the out-of-plane LC configuration both below and above the orientation transition. Figure 8 shows the pretilt angle averaged over the x-y plane, $\langle\theta\rangle_{xy}$, versus cell depth, z, for various λ between 0.2 μm and 1.6 μm. Clearly, the data demonstrate a jump of $\sim 40°$ in θ between

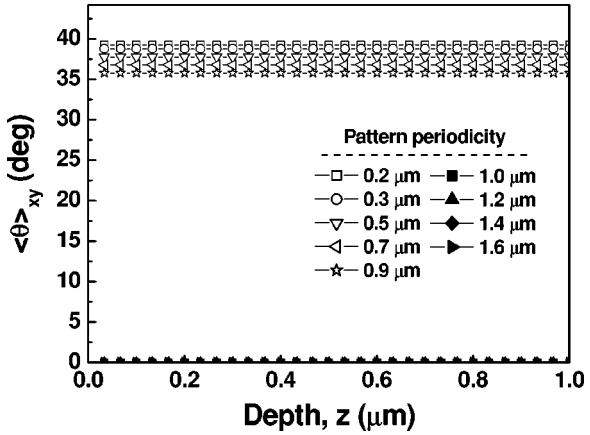

FIG. 8. Average pretilt over the *x*-*y* plane, $\langle\theta\rangle_{xy}$, versus depth *z* for various λ about the orientational transition.

λ=1 μm and λ=1.1 μm, in which the average pretilt is nearly a constant and equals ~40° and 0° for λ below and above the transition periodicity, respectively. Next we look at variation of the in-plane alignment of the LC with *z*. Shown in Fig. 9 are the plots of $\langle|\phi-\phi_0|\rangle_{xy}$ versus *z* for 0.2 μm $\leqslant\lambda\leqslant$1.6 μm. All curves exhibit monotonic decay toward the $\phi=45°$ direction in moving away from the substrate wall ($z=0$). But the average deviation of ϕ from ϕ_0 at the substrate is larger for smaller λ, and demonstrates a discontinuous jump when λ reaches the transition periodicity. Figure 9 also shows that, with larger periods, registration of ϕ with the local easy azimuthal direction can be maintained over a longer decay distance along ***z***. We fitted the data of Fig. 9 to $y_0+(45°-y_0)\exp(z/\ell_e)$ (where $y_0\equiv\langle|\phi-\phi_0|\rangle_{xy}$ at $z=0$ and ℓ_e is physically a decay length) and the results are displayed as solid lines in the same figure. Evidently, the model provides an excellent description of the data. In Fig. 10, we display the fitted values of ℓ_e as a function of λ. We found that the data fitted well to $\ell_e=0.086\lambda$ (solid line in Fig. 10). A previous calculation of Berreman [12], modeling the distortion of the LC director by a periodically corrugated surface topography, showed that the distortion should decay exponentially with a decay length equal to the period of the surface corrugation divided by 4π. Our current findings are consistent with this prediction.

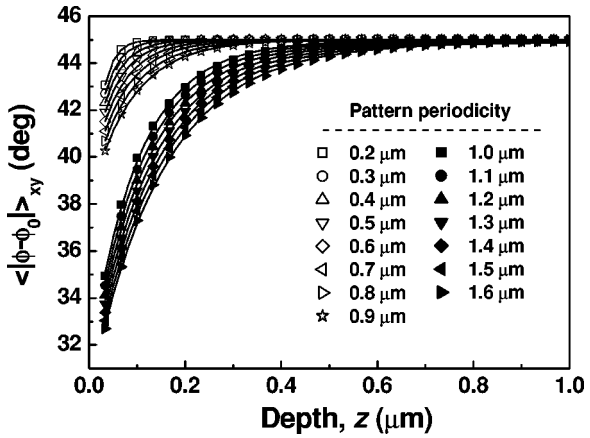

FIG. 9. Average of $|\phi-\phi_0|$ over the *x*-*y* plane, $\langle|\phi-\phi_0|\rangle_{xy}$, versus *z* for various λ about the orientational transition. Solid lines are fits to an exponential function (see text).

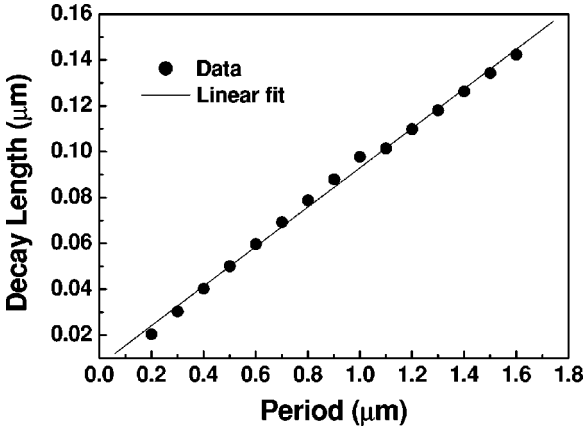

FIG. 10. Decay length deduced from data of Fig. 9 as a function of pattern periodicity. The solid line is a linear fit through the data points.

V. CONCLUDING REMARKS

From the results of this model shown above, the key to the observation of the LC orientation transition is a weak surface potential that allows large planar relaxations of the LC director toward the $\phi=45°$ direction to occur in the range of pattern periodicities studied. Moreover, the surface potential should possess a minimum at $\theta\approx40°$ as $\langle|\phi|\rangle$ approaches 45°. Should these two conditions be satisfied, the LC orientation transition can occur in two steps. First, the LC director homogenizes toward the $\phi=45°$ direction as λ is decreased. Then a jump in θ from 0° to 40° takes place to reduce the resulting increase in azimuthal energy. This result provides a natural reconciliation for the experimental findings of different groups. In particular, Kim *et al.* [4] did not observe the LC orientation transition in their experiment on checkerboard substrate patterns. It was, however, shown that the azimuthal anchoring energy of their substrates was quite high, $\approx1\times10^{-4}$ J m^{-2} [5], so that the extrapolation length for inhomogeneous anchoring in the plane ($\sim k_{11}/W_\phi$) was only ~0.064 μm, and significant planar relaxations of the LC director could not take place for the range of pattern periodicity examined ($\geqslant1$ μm). We also investigated the out-of-plane LC configuration. It is found that on either side of the transition any out-of-plane inhomogeneity relaxes exponentially away from the substrate in a manner consistent with the prediction of Berreman.

ACKNOWLEDGMENTS

We acknowledge financial support from the Research Grant Council of Hong Kong through Projects No. HKUST6133/97P, No. HKUST6150/01P, and No. HKUST6115/03E.

[1] H. L. Ong, A. J. Hurd, and R. B. Meyer, J. Appl. Phys. **57**, 186 (1985).
[2] T. Z. Qian and P. Sheng, Phys. Rev. Lett. **77**, 4564 (1996).
[3] B. Lee and N. A. Clark, Science **291**, 2576 (2001).
[4] J. Kim, M. Yoneya, J. Yamamoto, and H. Yokoyama, Mol. Cryst. Liq. Cryst. Sci. Technol., Sect. A **367**, 151 (2001).
[5] J. Kim, M. Yoneya, J. Yamamoto, and H. Yokoyama, Appl. Phys. Lett. **78**, 3055 (2001).
[6] J. Kim, M. Yoneya, and H. Yokoyama, Nature (London) **420**, 159 (2002).
[7] B. Zhang, F. Lee, O. K. C. Tsui, and P. Sheng, Phys. Rev. Lett. **91**, 215501 (2003).
[8] C. W. Oseen, Trans. Faraday Soc. **29**, 883 (1933); F. C. Frank, Discuss. Faraday Soc. **25**, 19 (1958).
[9] G. Barbero, T. Beica, A. L. Alexe-Ionescu, and R. Moldovan, J. Phys. II **2**, 2011 (1992).
[10] T. Z. Qian and P. Sheng, Phys. Rev. E **55**, 7111 (1997).
[11] H. Yokoyama and H. A. van Sprang, J. Appl. Phys. **57**, 4520 (1985).
[12] D. W. Berreman, Phys. Rev. Lett. **28**, 1683 (1972).
[13] A. Rapini and M. Papoular, J. Phys. (Paris), Colloq. **30**, C4-54 (1969).
[14] F. K. Lee, G. H. Wen, X. X. Zhang, and O. K. C. Tsui, J. Vac. Sci. Technol. B **21**, 162 (2003).
[15] J. D. Bunning, T. E. Faber, and P. L. Sherrell, J. Phys. **42**, 1175 (1981); T. Toyooka, G. Chen, H. Takezoe, and A. Fukuda, Jpn. J. Appl. Phys., Part 1 **26**, 1959 (1987).
[16] P. G. de Gennes, and J. Prost, *The Physics of Liquid Crystals* (Clarendon Press, Oxford, 1995).